COMPUTATIONS OF A FILM COOLED TURBINE ROTOR BLADE WITH NON-UNIFORM INLET TEMPERATURE DISTRIBUTION USING A THREE-DIMENSIONAL VISCOUS PROCEDURE

B. Weigand and S. P. Harasgama
Gas Turbine Development
ABB Power Generation Limited
Baden, Switzerland

ABSTRACT

A numerical investigation of film cooling on a turbine rotor blade has been carried out. The computations were performed with a 3D-Navier- Stokes code utilizing an unstructured solution adaptive grid methodology (Dawes (1992)). The code uses a low Reynolds number k-epsilon model for prescribing the Reynolds stresses. The results show that there is a significant interaction between the coolant flow and the secondary flow near the hub and the tip of the turbine blade. It was observed that, by blowing on the pressure side of the blade, some of the cooling air was transported through the tip gap of the blade to the suction side of the blade where the coolant flow interacts with the secondary flow field.

When radial inlet temperature distortion (RTD) is included, it was possible to show that there were some further modifications of the film cooling effectiveness on the rotating blade near the pressure side tip. This is believed to be mostly because of the changed secondary flow system due to the radial inlet temperature profile.

NOMENCLATURE

c_p	= specific heat at const. pressure
c	= axial chord length
CFL	= Courant-Friedrichs-Levy number
f_μ	= wall damping function $=1.-\exp(-0.008\,R_T)$
f_1	= wall damping function $=1.+(0.06/f_\mu)^3$
f_2	= wall damping function $=1.-\exp(-R_T^2)$
I	= rothalpy $=c_p T_{0rel}-0.5((\Omega r)^2)$
i_x, i_t, i_r	= unit vector components
k	= turbulent kinetic energy
LE	= leading edge
M	= blowing rate $=(\rho_c V_c/\rho_\infty V_\infty)$
Ma	= isentropic Mach number
$\dot{m}$	= mass flow rate
p	= pressure
p_{C0}	= absolute total pressure of the coolant
Pr	= Prandtl number
Pr_T	= turbulent Prandtl number
$\vec{q}$	= relative velocity $=V_x i_x+V_t i_t+V_r i_r$
R_T	= turbulent Reynolds number $=\rho k^2/\mu_{lam}\varepsilon$
r	= radial coordinate
t	= tangential coordinate
$\bar{t}$	= time
T	= temperature
T_G	= gas recovery temperature
T_C	= coolant recovery temperature
T_{C0}	= absolute total temperature of the coolant
T_{aw}	= adiabatic wall temperature
TE	= trailing edge
U	= wheel speed $=\Omega r$
V_r, V_t, V_r	= velocity components
ε	= turbulent dissipation
η	= film cooling effectiveness $=(T_C(x=0)-T_\infty)/(T_G(x=0)-T_c)$
λ	= effective heat conductivity $=c_p(\mu_{lam}/\mathrm{Pr}+\mu_T/\mathrm{Pr}_T)$
μ	= effective dynamic viscosity $=\mu_{lam}+\mu_T$
μ_{lam}	= molecular dynamic viscosity
μ_T	= turbulent dynamic viscosity $=\rho f_\mu c_1 k^2/\varepsilon$
θ	= angle in tangential direction
ρ	= density
$\bar{\bar{\sigma}}$	= stress tensor
Ω	= rotation speed

Subscripts

aw	= adiabatic wall
C	= coolant
G	= gas
HUB	= near the hub
p	= pressure side
s	= suction side
TIP	= near the tip
∞	= free stream conditions
0	= absolute total quantities

Presented at the International Gas Turbine and Aeroengine Congress and Exposition
The Hague, Netherlands — June 13–16, 1994

Superscripts

^	= maximum value
v	= minimum value
-	= vector

INTRODUCTION

The desire for higher thermal efficiency of gas turbines has led to increases in turbine entry temperature. The present high level of turbine entry temperature necessiates the efficient cooling of the first stage turbine blading. One such method is film cooling by injection of cooling fluid through rows of holes, and this method is now widely used in practice.

During the last thirty years the parameters affecting film cooling have been extensively studied. An excellent survey of the work up to 1971 can be found in Goldstein (1971). More recent surveys can be found in Louis (1977) and in Jones(1986). These reviews contain studies concerned, for example, with the effect of the shape of the holes, the change in blowing rate, momentum flux ratio and density ratio on the film cooling effectiveness.

There are, however, very little film cooling data on rotating blades because of the difficulty of direct measurement of film cooling effectiveness on such components. Dring et al. (1980) studied the film cooling effectiveness and trajectories of the coolant blowing through a single hole on the pressure side and on the suction side of a large scale, low-speed rotor blade model. They found that the results agreed well with Ito et al. (1978) for stationary cascade data for the suction side of the blade, while they observed quite different shapes of the trajectories on the pressure side of the blade because of rotational effects acting on the coolant flow.

Takeishi et al. (1992) measured the film cooling effectiveness on a low-speed stationary cascade and also on a rotating blade by using a heat-mass transfer analogy. They found that the film cooling effectiveness on the suction side of the blade fits well with that on the stationary blade, but a lower level of effectiveness appears on the pressure surface of the rotating blade.

To the best knowledge of the authors there exists no numerical study dealing with three-dimensional film cooling on a rotating turbine blade. Therefore, the subject of the present paper is to present a computational study on the three-dimensional effects occurring on a film cooled rotor blade. The study is limited to the case of blowing in the tangential direction, but nevertheless, the paper hopes to help advance our understanding of the very complicated features of this type of flow.

The radial temperature distortion at the inlet to a rotating turbine rotor was found to have a remarkable influence on the secondary flows and the heat flux at the surface (Harasgama (1990)). Since the secondary flow field can affect the hydrodynamics of the film coolant, the effect of RTD on film effectiveness is also presented.

THE NUMERICAL APPROACH

The results presented in this paper were obtained with a 3D-Navier-Stokes code written by Dawes (1992). The program will be only briefly described in this paper. For more detailed information the reader is referred to Dawes (1993).

The equations solved are the fully 3D Reynolds-averaged Navier-Stokes equations expressed in strong conservation form and retaining the full stress tensor including the full viscous energy equation. The time averaged Reynolds stresses are resolved by using a low Reynolds number k-epsilon model (Patel et. al (1985)). In a right handed cartesian (X,T,R) coordinate system rotating with speed Ω about the x-axis the equations of motion are

$$\frac{\partial}{\partial \bar{t}} \oint_{Vol} \bar{F}\, dVol = \oint_{Area} \bar{H}\, dArea + \oint_{Vol} \rho \bar{S}\, dVol \qquad (1)$$

where

$$\bar{F} = [\rho, \rho V_x, \rho V_t, \rho V_r, \rho E, \rho k, \rho \varepsilon]$$

$$\bar{H} = \begin{bmatrix} \rho\bar{q} \\ \rho\bar{q}V_x + \bar{\bar{\sigma}}i_x \\ \rho\bar{q}V_t + \bar{\bar{\sigma}}i_t \\ \rho\bar{q}V_r + \bar{\bar{\sigma}}i_r \\ \rho\bar{q}I + \bar{q}\cdot\bar{\bar{\sigma}} + \lambda\nabla T \\ \rho\bar{q}k + (c_2\mu/\rho)\nabla k \\ \rho\bar{q}\varepsilon + (c_3\mu/\rho)\nabla \varepsilon \end{bmatrix} \quad \bar{S} = \begin{bmatrix} 0 \\ 0 \\ r\Omega^2 - 2\Omega V_r \\ r\Omega^2 - 2\Omega V_t \\ 0 \\ G - \rho\varepsilon \\ f_1 C_4 \varepsilon G/k - f_2 C_5 \rho\varepsilon^2/k \end{bmatrix} \qquad (2)$$

where $\bar{\bar{\sigma}}$ is the stress tensor with the definition $\bar{\bar{\sigma}} = -p\bar{\bar{I}} + \bar{\bar{\tau}}$, $\bar{\bar{\tau}} = 2\mu\, def(\bar{q}) - 2/3(\mu(\nabla\bar{q})\bar{\bar{I}})$, $def(\bar{q}) = 1/2(\nabla\bar{q} + (\nabla\bar{q})^T)$ and the function $G = 2\mu(def(\bar{q}))^2 - 2/3(\mu(\nabla\bar{q})^2)$. For further details of the numerical approach the reader is referred to Dawes (1993).

Geometry and computational mesh

Fig. 1 shows the geometric model for the internal cooling system, which was used for the present investigation. From the figure, which shows a mid-span section, it can be seen that only the case of blowing in tangential direction was studied. For the present paper, only the basic physics of the filmcooling

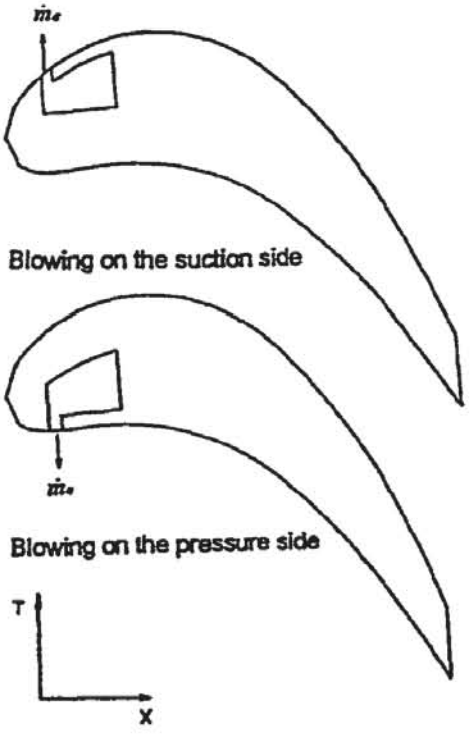

Fig. 1 Geometric model for the internal cooling system.

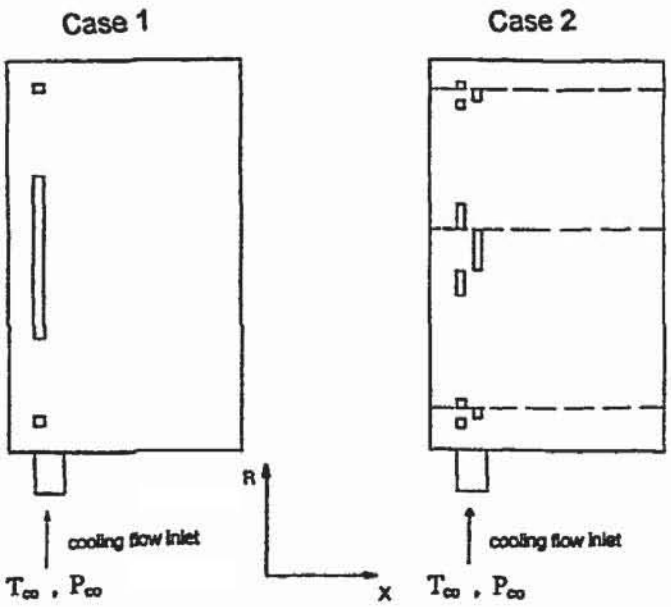

Fig. 2 Blade film cooling geometry.

interactions on a rotating blade was modelled with and without RTD. Therefore it was thought that modelling the case of blowing in tangential direction was sufficient to illustrate the film cooling hydrodynamics. Currently work is carried on to represent also the case of blowing under an arbitrary angle to the surface. Fig. 2

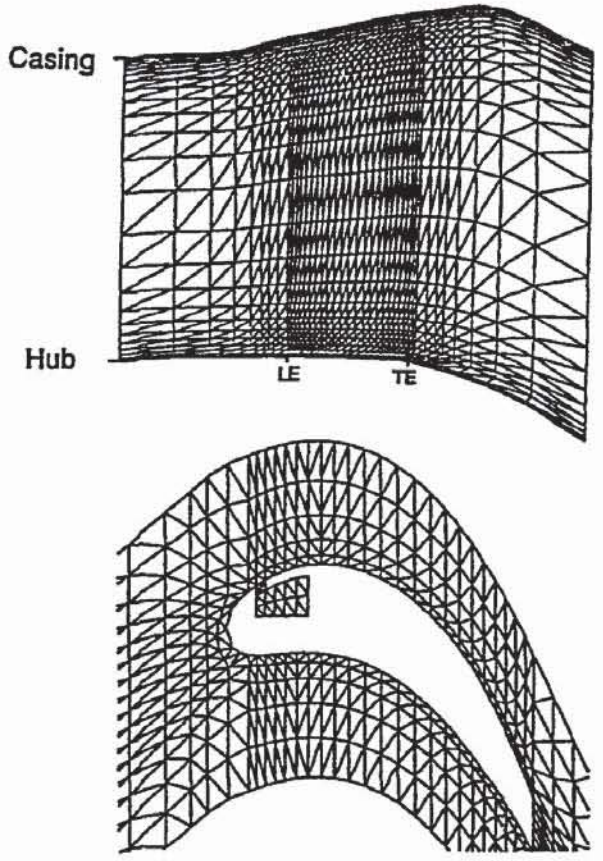

Fig. 3a The basic unstructured mesh with 73056 cells and 15014 nodes.

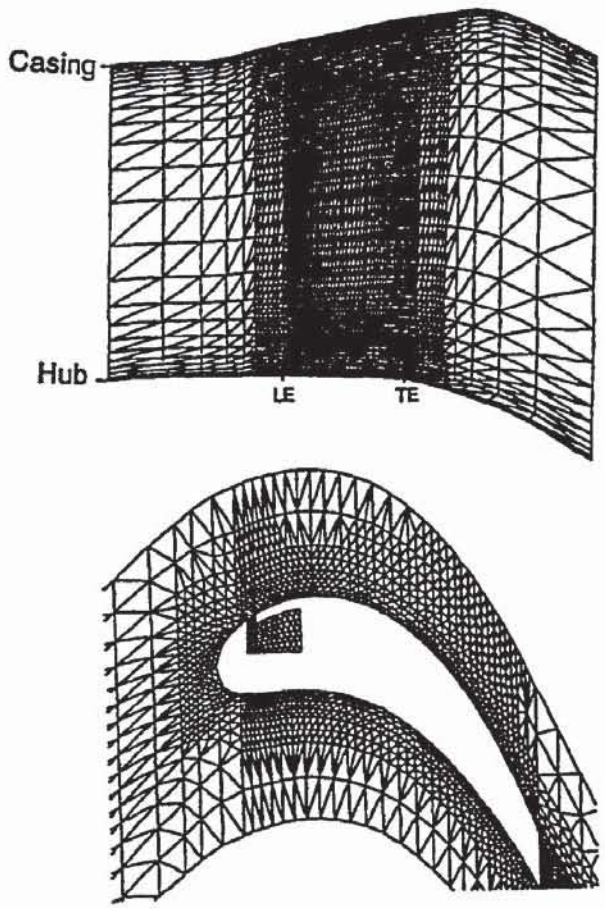

Fig. 3b The unstructured messh after refinement with 358169 cells and 67281 nodes.

shows the two different blowing geometries which were taken into account. Case one shows a single slot located at mid-span and two single holes near the hub and the tip of the blade. This simple configuration was chosen to show the basic mechanism of radial deflection of the outcoming coolant flow due to the outer pressure distribution. Case 2 can be considered to display the real situation more closely. This model allows mixing between the individual outcoming coolant flows. Further it is possible to see the interaction between the coolant flow and the flow over the tip gap more clearly.

The calculations were started on a coarse grid with only 17 grid points in tangential direction, 29 points in radial direction and 46 points in axial direction (see Fig. 3). This results in a total number of tetrahedral cells of about 73 000 with about 15 000 individual nodes. As it can be seen in Figs. 1-3, due to the limited number of grid points in axial and tangential direction, the representation of the leading edge and of the trailing edge of the blade is somewhat crude. The present study was to examine the influence of RTD and rotation on the film cooling effectiveness. Consequently, it was not thought to be necessary that a accurate representation of the leading edge and the trailing edge would be required in order to capture the fundamental physics of the process. Also, by doing some calculations for the uncooled blade with a structured 3D-Navier-Stokes code, Dawes (1986), (with 30 grid points in radial direction, 30 grid points in tangential direction and 100 grid points in axial direction) it was observed that the aerodynamics of the profile as well as the mass flow rate were still preserved quite well with the present representation of the leading and trailing edge of the blade.

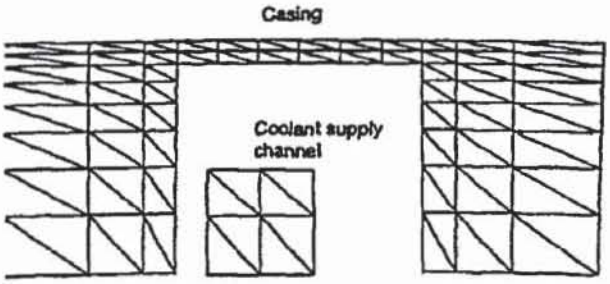

The basic unstructured mesh

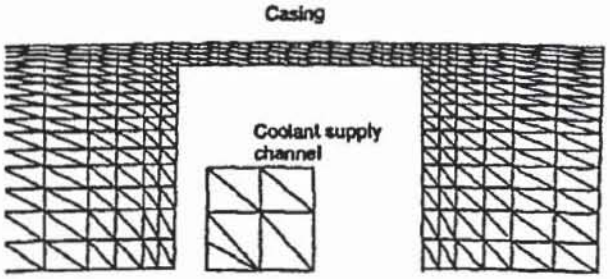

The unstructured mesh after refinement

Fig. 3c The mesh in the tip gap for an axial cut at 14% axial chord.

For the coarse grid a converged solution was obtained with a total mass error smaller than 1%. After reaching a converged solution for the coarse grid, the initial grid was refined using different refinement strategies resulting in a total number of about 358 000 cells associated with 67 000 nodes. Special care had to be taken in doing this refinement. It was found to be necessary to refine the grid in the coolant slots and in the channel which supplies the coolant fluid. This is because of the influence of the outer flow on the flow in the supply channel. This means that the influence of the outer pressure field at the film cooling location determines the incoming coolant mass flow in the coolant supply channel. This effect is covered better if the coolant channel and the coolant slots are refined well so that the viscous flow in this area can be resolved correctly.

Boundary conditions and solution algorithm

Boundary conditions were applied at all six sides of the three-dimensional solution domain. For the inflow boundaries the total pressure, the total temperature, the turbulent kinetic energy, the dissipation rate and two flow angles have to be prescribed, while at the outflow boundaries the static pressure is specified. The hub, the tip and the casing were considered to be viscous boundaries, while periodicity conditions were applied for the two tangential gridlines which are the boundaries of the computational domain. Because the values of the total temperature and the total pressure have to be prescribed at the inlet of the coolant flow into the system, the blowing rate, for example, is obtained as a result of the calculations.

The solutions were performed with adiabatic wall boundary conditions in order to obtain the film cooling effectiveness.

The net flux imbalance into each cell is used to update the flow variables themselves via a four-step Runge-Kutta time marching scheme with residual smoothing. Residual smoothing is applied after each fractional time step to extend the stability domain of the algorithm. For the present study the code was run with a constant CFL (Courant-Friedrichs-Levy) number of 2.5 imposed everywhere in the flow field. This corresponds with a spatially varying time step. The values of the constants for the smoothing terms were selected as the minimum possible values for which small "wiggles" were observed in the solution. This was done in order to keep the influence of this term on the final solution as small as possible.

It was assumed that convergence of the solution was achieved, when the relative deviation between the inlet and the exit mass flow was less than 1%. It was not possible to reach relative deviations between the inlet and the exit mass flow smaller than 0.5%, because of the strong blowing in tangential direction, causing a strong disturbance of the outer flow field. In addition, the RMS (root mean square) of the rate of change of density over the current time step and the entire flow domain ($Vol\partial\rho/\partial\tilde{t}$) was checked to verify convergence. Experience shows that typically this value must decay by three - to four orders of magnitude to obtain convergence. For the present solution, this was the case.

The CPU time for obtaining a fully converged solution was approximately 45 hours on a Hewlett Packard (HP 9000/750) workstation.

By refining the grid for the present case only partial use could be made of the unstructured grid methodology. This was mainly because of the interest of the present paper on the film cooling effectiveness, which is a quantity which has to be evaluated at the blade surface. Consequently, the current results were obtained by refining the initial coarse grid near the blade surface, in the coolant supply channel, the coolant slots and near the tip gap. Additionally, the grid was refined using the cellwise change of entropy as an indicator. By using several levels of grid refinement the solution was converged to a grid independent one. Only these are presented in this paper.

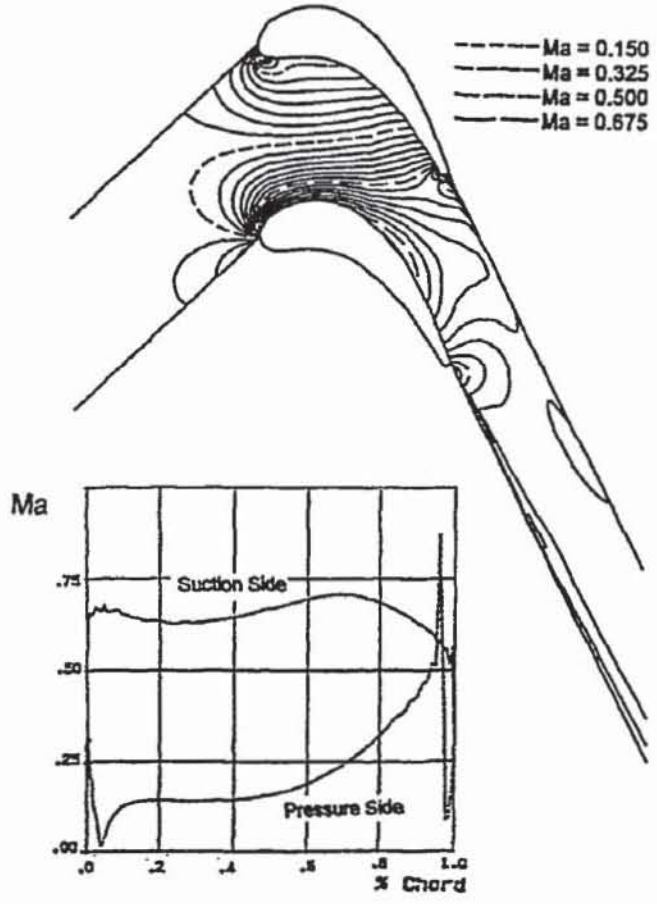

Fig. 4 Distribution of the isentropic Mach number at mid-span.

RESULTS AND DISCUSSION

Rotor Aerodynamics

The rotor blade aerodynamics are presented in Fig. 4. The figure shows the distribution of the isentropic Mach number on the suction side and on the pressure side of the uncooled rotor blade. The tip clearance was taken to be 1% of the span for all the calculations.

The main design parameters of the turbine are given below:

Work capacity ($C_P \Delta T / T$)	:97 (J/kg K)
Blade Speed ($U/\sqrt{T}$)	:7.9 (m/s $\sqrt{K}$)
Aerodynamic Loading ($\Delta h / U^2$)	:1.56
Pressure Ratio (Total-to-static)	:1.52
Flow Coefficient (V_a/U)	:0.54
Pitch/ Chord Ratio	:1.02
Aspect Ratio	:2.27
Mean Rotor Hub / Tip Ratio	:0.81
Flow Function ($\dot{m}\sqrt{T} / P$)	:0.0176 ($\sqrt{K}$ m s)

Film Cooling Results

First of all, it is interesting to visualize the principal differences which are present between blowing on the suction side and on the pressure side of the blade. Fig. 5 shows distributions of the relative stagnation temperature for the simple geometric case 1. The blowing rate M was approximately 1 for both cases. The ratio of coolant mass flow to the mass flow rate in the main flow was 1.3%. The value for the total temperature of the coolant is indicated in the figure. At the inlet of the rotor a constant total temperature of 1400 K was applied. The differences existing in the shape of the isotherms are quite obvious. It can be seen that for blowing on the suction side the isotherms around the central slot are not deflected in the radial direction. Because the results were obtained with adiabatic wall boundary conditions, the shape of the relative total temperature at the wall corresponds closely to the shape of the film cooling effectiveness. The shape of the film cooling effectiveness on the suction side of the blade are typical for the distribution of η for non - rotating cases.

The situation is quite different if blowing on the pressure side of the blade is considered. It can be observed that the surface trajectories show a strong radial displacement. The reason for this radial deflection of the isotherms was theoretically shown by Hawthorne (1974) and subsequently confirmed experimentally by Dring and Joslyn (1983) to be the relative eddy. In their paper, Dring and Joslyn (1983) derived under the assumption of free vortex flow at the rotor inlet a equation for the relative radial velocity given by

$$\left(\frac{V_r}{U}\right)_p = (\theta_p - \theta_s) \qquad (3)$$

Because the relative axial velocity on the pressure side is much smaller than on the suction side of the blade, the radial deflection of the isotherms appearing on the pressure side of the blade is much more pronounced than on the suction side.

It is interesting to note that Dring et al. (1980) obtained qualitatively the same shape of trajectories in their experiment (Fig. 6). They observed experimentally that there is nearly no difference in the shape of the trajectories if the blowing rate is changed. We were able to confirm this statement by performing computations with different blowing rates for the shown geometry. The reason that Dring et al. (1980) could not see any differences in the shape of the trajectories was because they investigated only one single hole located at mid-span. For a film cooling hole located near the hub or the tip of the blade, there is a difference in the shape of the trajectories for various blowing rates, as will be shown later.

Fig. 7 shows the distribution of the film cooling effectiveness at mid- span. The film cooling effectiveness is defined in the present paper by

$$\eta = \frac{T_G(x=0) - T_\infty}{T_G(x=0) - T_c} \qquad (4)$$

The recovery temperature T_G of the main gas flow was taken for

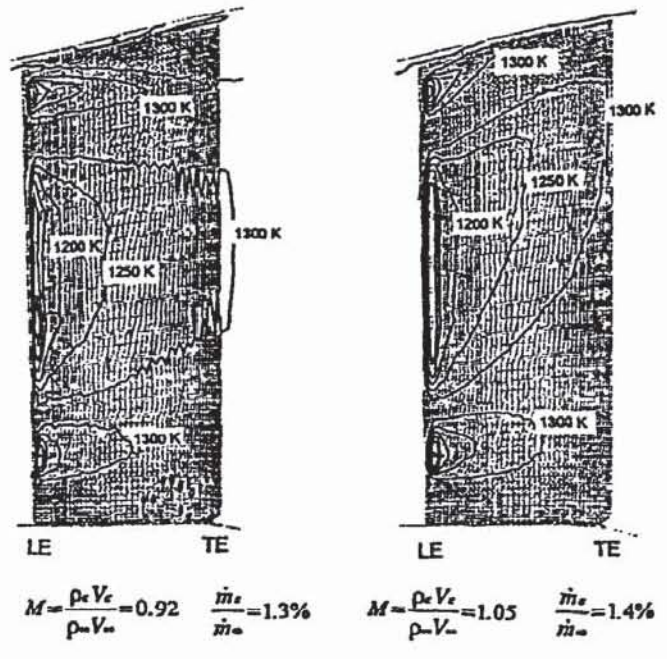

Fig. 5 Distribution of the relative total temperature at the blade surface (Case 1 geometry) for $T_{G0}(x=0) = 1400\,K$ and $T_{C0} = 800\,K$.

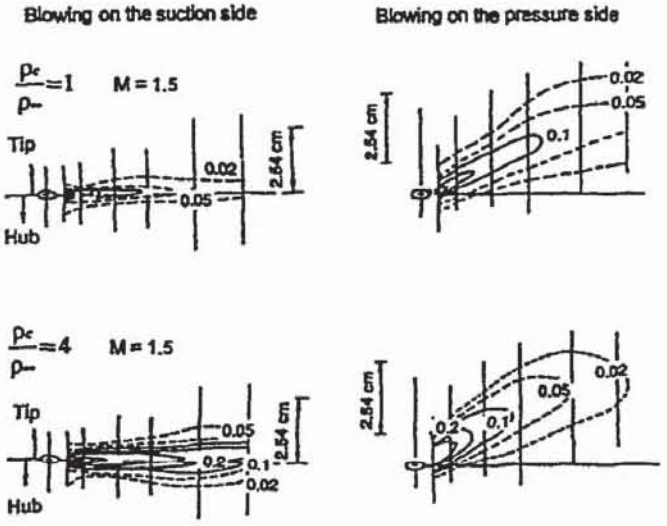

Fig. 6 Measured distributions of the film cooling effectiveness on the blade surface according to Dring et al. (1980).

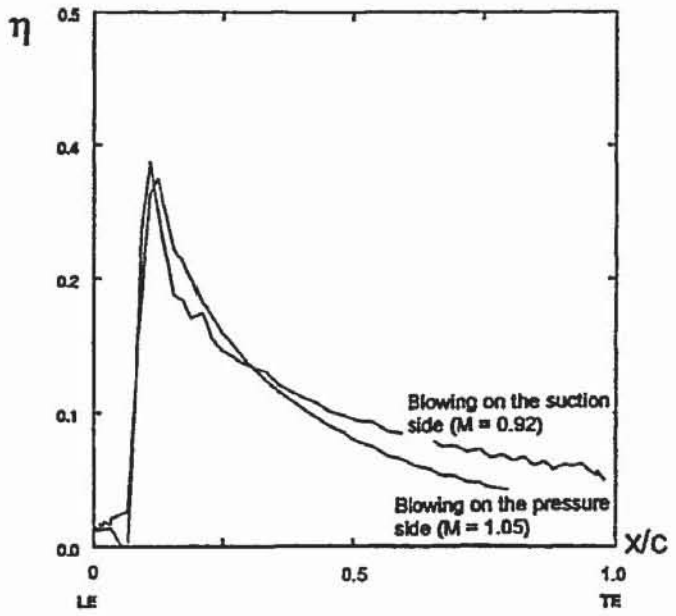

Fig. 7 Computed film cooling effectiveness at mid-span.

the same radial value where the film cooling effectiveness was shown, but at the inlet (x=0). This definition was used with regard to the case of radial temperature distortion at the inlet, which will be discussed later.

It can be seen from Fig. 7 that the film cooling effectiveness on the pressure side of the blade decays more rapidly than on the suction side of the blade for the same blowing rate. Dring et al. (1980) observed a more pronounced difference in the film cooling effectiveness between the pressure side and the suction side of the blade. This is believed to be caused by the inclined holes they used (30° to the local surface) in their experiment resulting in a much lower film cooling effectiveness very near to the injection point for blowing on the pressure side. For the present case of blowing in tangential direction the film cooling effectiveness reaches nearly the same values close to the injection point for either blowing on the pressure or on the suction side of the blade. This is due to the reason that the

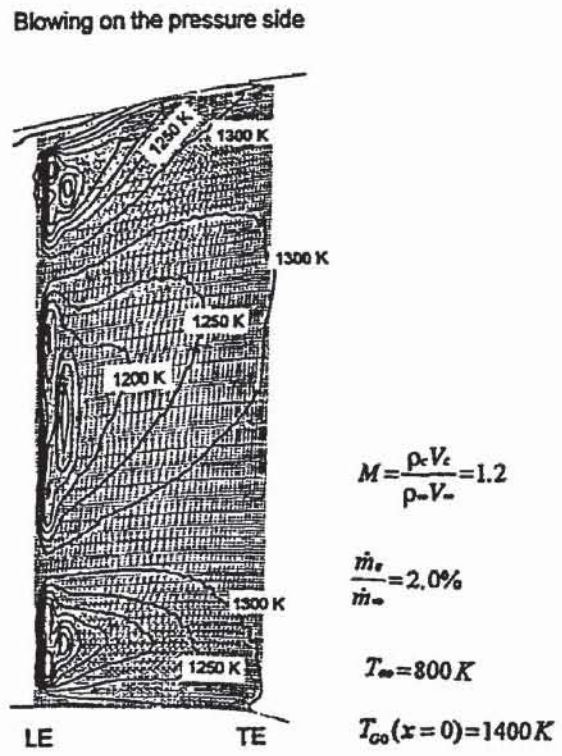

Fig. 9 Distribution of the relative total temperature at the pressure side of the blade (Case 2 geometry).

coolant penetrates the edge of the boundary layer (blowing in tangential direction). Therefore, the wall curvature is in this case not of strong influence, which is quite different to the geometric case Dring et al. (1980) studied. This explains the smaller difference in the film cooling effectiveness between blowing on the pressure side and on the suction side of the blade for blowing in tangential direction.

As stated above, the simple first geometry given in Fig. 2 can only display some mechanisms which are present. To get a more realistic insight into the physical mechanism taking place in

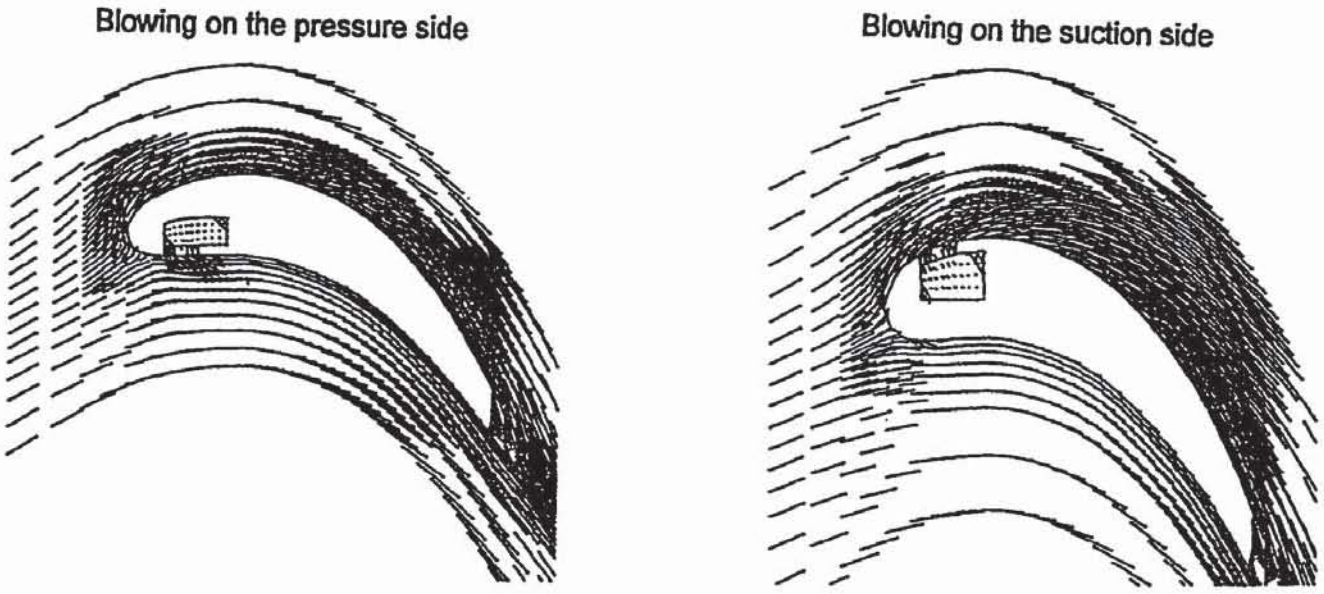

Fig. 8 Visualization of the flow field for a radial cut near mid-span.

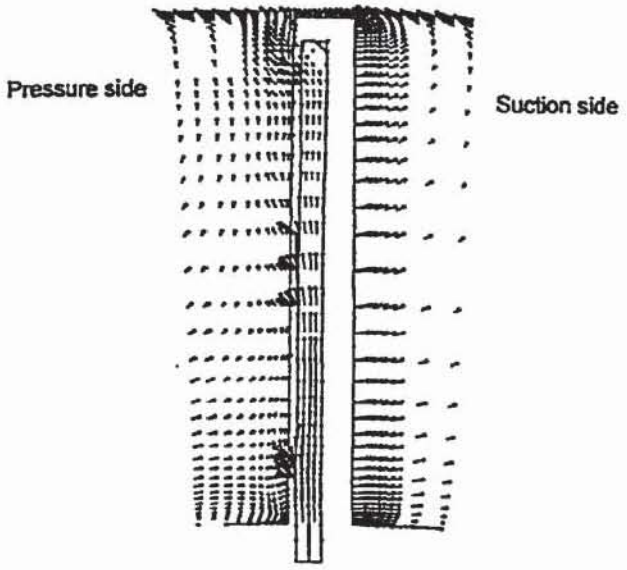

Fig. 10 Relative velocity vectors for an axial cut at 16% axial chord (Case 2 geometry).

the real turbine, the second geometry shown in Fig. 2 was studied extensively. Fig. 8 shows the velocity vectors around the blade for a slice for a constant rotor blade radius with blowing on the suction side and on the pressure side of the rotor blade. It can be seen that the coolant flow, penetrating the external region in the tangential direction, is deflected by the outer flow field. Fig.9 shows the distribution of the relative total temperature on the pressure side of the blade for a blowing rate of M=1.2. The influence of the coolant flow on the temperature distribution at the blade surface can be clearly detected. Also the mixing of the coolant flows from the individual holes can be observed in this figure, because the mixing process results in a changed shape of the isotherms close to the injection holes. The isotherms around

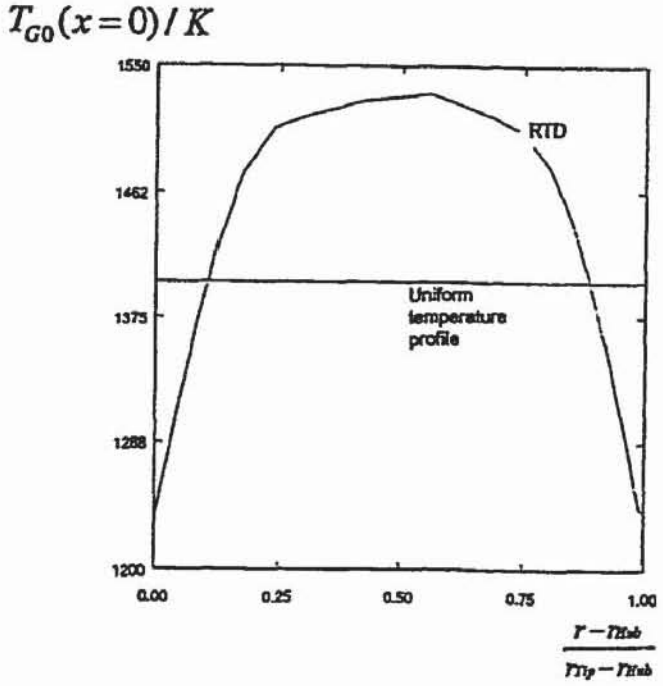

Fig. 11 Distribution of the absolute total temperature at the inlet of the rotor blade.

the upper three holes are strongly deflected because of the strong secondary flow field in this region. It can be seen that some of the coolant flow penetrates the tip gap and is therefore transported to the suction side of the blade. To visualize this effect in more detail, Fig. 10 shows the relative velocity vectors for an axial cut at 16% axial chord. From this figure it can be seen that the film coolant flow is transported through the tip gap to the suction side of the blade. Also, it can be observed that the coolant flow penetrating through the tip gap interacts on the suction side of the blade with the established secondary flow field. This gives a good impression how complicated and three-dimensional the problem of film cooling on a rotor is in this region.

Effect of Radial Temperature Distortion

To study the effect of RTD on the aerodynamics and on the film cooling effectiveness on the rotating turbine blade, several computations were made with the second geometry shown in Fig. 2. For the present simulations the radial temperature distribution at the inlet of the computational domain was approximated by a uniform parabolic profile shown in Fig. 11. As can be seen from this figure, the ratio of the maximum total temperature to the minimum total temperature at the inlet is 1.2. This ratio can take larger values in some cases (Harasgama (1990) investigated a ratio of 1.4). Nevertheless, this would result in the same type of effects shown in the present paper.

The inlet to the rotor blade in the actual turbine will be an unsteady temperature field. Also there will be a rather complicated time dependent interaction between the outcoming cooling flow and the time dependent external temperature field. However, for the purpose of establishing the mean heat load to the rotor a simulation may be achieved by a radial temperature profile being imposed ahead of the rotor. This method is of design significance because in an engine the thermal diffusivity of the metal rotor blade will average out the unsteady features in the flow field. A simulation using a three-dimensional viscous

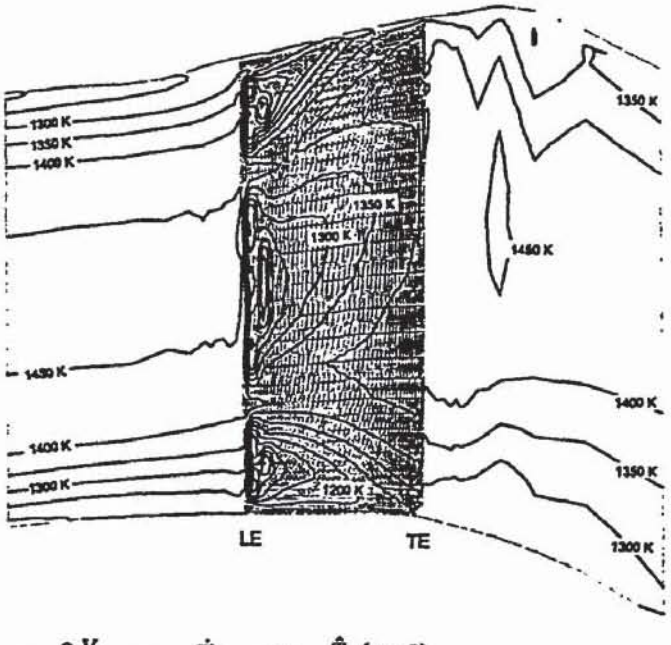

Fig. 12 Relative total temperature for a tangential cut at the pressure side of the blade (Case 2 geometry).

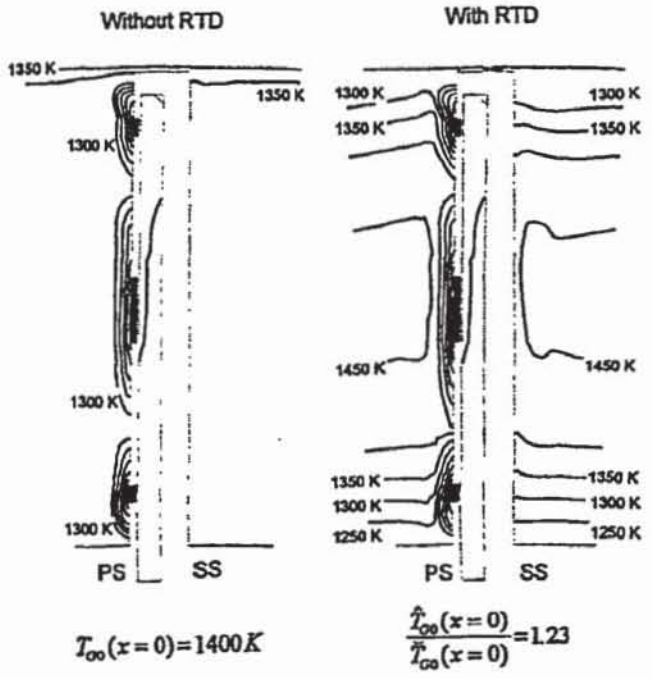

Fig. 13 Comparison of the distribution of the relative total temperature with and without RTD for an axial cut at 16% axial chord (Case 2 geometry, M = 1.2, $\dot{m}_C/\dot{m}_{\infty}=2.0\%$ and $T_{C0}=800K$).

code should therefore provide useful insight in to the physics of the flow within a cooled turbine rotor with inlet temperature distortion.

Fig. 12 shows the distribution of the relative stagnation temperature on the pressure side of the blade for a blowing rate M = 1.2 for the case of a radially distorted temperature profile at inlet. This figure corresponds with Fig. 9. By comparing the two figures it can be observed that the radial temperature distortion increases the secondary flow effects, resulting in a quite different shape of the isotherms near the hub and tip of the blade. From the two figures it is quite obvious that the effect of RTD on the shape of the isotherms is more pronounced near the tip of the blade. This result agrees with the observations made by Harasgama (1990).

Fig. 13 compares the shape of the isotherms for an axial cut at 16% axial chord for the case with and without radial temperature distortion. Both plots show the region of influence of the film cooling flow on the external flow field. Because the change of the external aerodynamics due to RTD is small (Harasgama (1990)) the region of influence of the cooling flow is nearly the same for both cases.

It is of special interest for the designers to see the difference in film cooling effectiveness for various blowing rates. Fig. 14 and Fig. 15 show the distribution of the film cooling effectiveness for three different radial positions. These positions are indicated in Fig. 2. While Fig. 14 shows the situation for a blowing rate M = 0.53, Fig. 15 displays the situation for the higher blowing rate M = 1.2. The distribution of η at mid-span shows clearly that there is no big difference in the film cooling effectiveness for the different blowing rates. It can be seen that the curves with and without RTD nearly coincide, which indicates that the influence of the radial inlet temperature distortion effects the shape of the isotherms only parametrically. This means that the secondary flow field is not changed due to RTD in this region. Near the hub of the blade the change in blowing rate results in a more pronounced increase in film cooling effectiveness. It is interesting that also near the hub of the blade there is no big difference in the shape of the film cooling effectiveness with and without RTD. This indicates that the changes in the flow field due to RTD are not so pronounced (see also Fig. 9 and Fig. 12) for both radial positions.

More pronounced differences due to the effect of RTD can be observed near the tip of the blade. The differences which can be observed are mainly caused by the different deflection of the isotherms in the cases with and without RTD due to changed secondary flows. In this figure it can be seen that the film cooling effectiveness η takes values lower than zero for the case of RTD. This is caused by using T_G at x = 0 in the definition of the film cooling effectiveness.

CONCLUSIONS

This paper shows results of a computational study of 3D-film cooling on a rotating turbine blade. Only the case of blowing in tangential direction was investigated.

It was shown with the present numerical model that large differences exist in the shape of the film cooling trajectories on the pressure side and on the suction side of the blade. Blowing on the pressure side of the blade resulted in some of the coolant

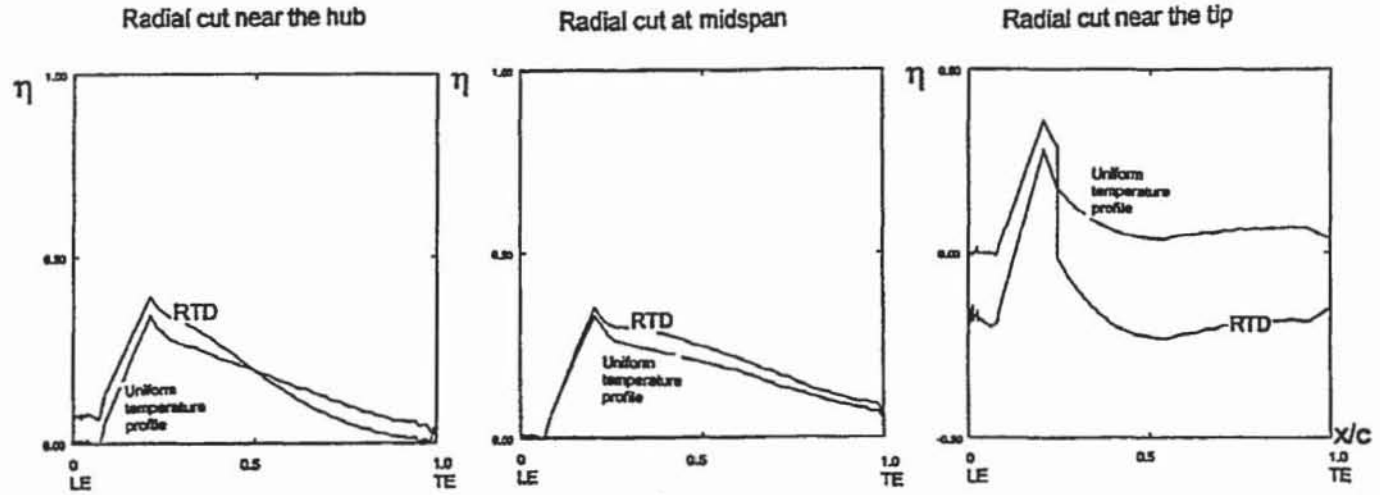

Fig. 14 Axial variation of the film cooling effectiveness for M = 0.53 for various radial positions indicated in Fig. 2 (blowing on the pressure side).

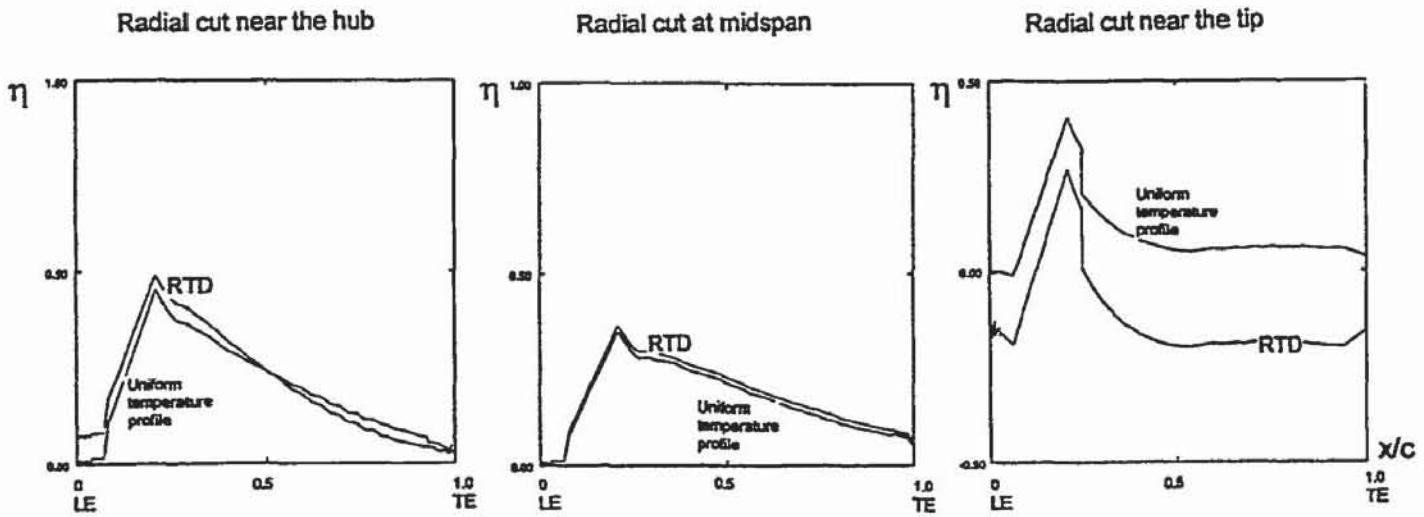

Fig. 15 Axial variation of the film cooling effectiveness for M = 1.2 for various radial positions indicated in Fig. 2 (blowing on the pressure side).

flow being transported through the tip gap of the blade to the suction side.

It was shown that the effect of RTD on the film cooling effectiveness is most significant near the tip of the blade. At the hub and near mid-span of the blade the curves for the film cooling effectiveness are very similar with and without RTD.

These results agree very well with the results reported by Harasgama (1990) who investigated the effect of RTD on the aerodynamics and on the heat transfer of a rotating turbine blade.

Unfortunately, there are no measurements available which deal with the case of blowing in tangential direction. Further work is planned to recalculate the case of blowing under an arbitrary angle to the surface of the blade for which measurements of the film cooling effectiveness are available.

ACKNOWLEDGEMENT

The authors kindly acknowledge the help and the interesting discussions with Dr. W.N. Dawes concerning the calculations and results presented in this paper. The authors also wish to thank ABB Power Generation Ltd for permission to publish this paper.

REFERENCES

Dawes W.N. (1986), "A numerical method for the analysis of three dimensional viscous compressible flow in turbine cascades: application to secondary flow development in a cascade with and without dihedral", ASME 86-GT-145.

Dawes W.N. (1992), "The extension of a solution-adaptive 3D Navier-Stokes solver towards geometries of arbitrary complexity", ASME 92-GT-363, to be published in ASME J. Turbomachinery.

Dawes W.N. (1993), "The practical application of solution-adaption to the numerical simulation of complex turbomachinery problems", Progess in Aerospace Sciences, Vol. 29, No.3, pp. 221-269.

Dring R.P. and Joslyn H.D. (1983), "The relative eddy in axial turbine rotor passages", ASME 83-GT-22.

Dring R.P., Blair M.F. and Joslyn H.D. (1980), "An experimental investigation of film cooling on a turbine rotor blade", ASME J. of Engineering for Power, Vol. 102, pp. 81-87.

Goldstein R.J. (1971), "Film cooling", *Advances in Heat Transfer*, Academic Press, New York and London, Vol. 7,pp. 321-379.

Harasgama S.P. (1990), "Combustor exit temperature distortion effects on heat transfer and aerodynamics within a rotating turbine blade passage", ASME 90-GT-174.

Hawthorne W.R. (1974), "Secondary vorticity in stratified compressible fluids in rotating systems", University of Cambridge , Dep. of Engineering, Report: CUED / A-Turbo / TR 63, June 1974.

Ito S., Goldstein R.J. and Eckert E.R.G. (1978), "Film cooling of a turbine blade", ASME J. Engineering for Power, Vol. 100, pp 476-481.

Jones T.V. and Forth C.J.P. (1986), "The scaling of film cooling: Theoretical and experimental results", Convective Heat Transfer and Film Cooling in Turbomachinery, von Karman Institute for Fluid Dynamics, Lecture Series 1986 - 06, pp. 1-30.

Louis J.F. (1977), "Systematic studies of heat transfer and film cooling effectiveness", High Temperature Problems in Gas Turbine Engines, AGARD CP-229, Paper 28, Ankara, Turkey.

Patel V.C., Rodi W. and Scheuerer G. (1985), "Turbulence models for near wall- and low Reynolds number flows: a review", AIAA Journal, Vol. 23. No. 9, pp 1308-1319.

Takeishi K., Aoki S., Sato T. and Tsukagoshi (1992), "Film cooling on a gas turbine rotor blade", ASME J. of Turbomachinery, Vol. 114, pp. 828-834.